

# A Time-Reversal FDTD Method for Image Reconstruction in the Presence of Noise

Ayed R. AlAjmi and Mohammad A. Saed

Department of Electrical Engineering  
Texas Tech University, Lubbock, TX 79409, USA  
ayed.alajmi@ttu.edu, mohammad.saed@ttu.edu

**Abstract** — A new method for image reconstruction using the time-reversed finite-difference time-domain method (TR-FDTD) in severely noisy environments is presented. The proposed method combines cross-correlation processing with TR-FDTD to successfully produce clear images even in the presence of large amount of noise in the captured signals. The method's capabilities are demonstrated through simulations and experiments in the x-band frequency region (8-12 GHz). Behind the wall imaging was used as a test case to validate the method. Numerical and experimental noise were added to corrupt the signals, and images were reconstructed with and without the added noise. The proposed method successfully produced clear images while the standard TR-FDTD method resulted in unrecognizable images. The efficacy and robustness of the proposed technique make it promising for applications including through-wall and buried-objects imaging in noisy environments.

**Index Terms** — Cross-correlation, FDTD, microwave imaging, time reversal.

## I. INTRODUCTION

Microwave imaging techniques have attracted extensive attention because of their remarkable advantages in many applications, such as military radar, surveillance radar, and security screening [1-3]. Given their non-destructive nature on human tissues, microwave-imaging techniques are currently the subject of extensive research for medical imaging applications such as the early detection and diagnosis of breast tumors [4-6]. Microwave frequencies can also penetrate different kinds of barriers, and this feature makes them an excellent candidate for through-wall imaging [7, 8]. Significant improvements were made in the last decade in the field of microwave imaging. Some of these improvements include the confocal microwave imaging algorithm for detecting and localizing breast tumors [9]. In [10], an imaging technique based on the microwave holography was proposed for breast cancer detection. The time reversal of electromagnetic waves for imaging was introduced by

Lerosey et al. [11]. The concept of time-reversal imaging algorithms relies on recording scattered signals from objects with the use of transducers and then re-emitting these signals by back-propagation into the same medium to refocus them on the source. It was first proposed in acoustics and ultrasound application [12]. In [13], a numerical study of time-reversed ultra wide-band (UWB) electromagnetic waves in continuous random media was conducted. New techniques for detecting and tracking moving targets in clutter with the use of a UWB time reversal method were investigated in [14]. Microwave breast cancer location detection using the finite difference time domain method (FDTD) with time-reversal technique was proposed in [15]. This method is based on the solutions to the time-dependent Maxwell's curl equations, which are represented as discrete formulas in time and space under a time reversal scheme to reconstruct images from previously captured data. Recently, a computationally efficient method for three-dimensional time-reversal FDTD microwave imaging technique was developed to successfully obtain detailed images of a simulated scattering object [16]. The optimum time frame to reconstruct images using this time stepping method is an important problem to which several solutions have been suggested in the literature [17-19].

Although imaging with microwave frequencies has a promising potential, the main challenge involved is the vulnerability of this range of frequencies to environmental noise that might eventually distort imaging results. In this paper, we present a novel microwave imaging technique based on the TR-FDTD method incorporating cross-correlation processing to minimize the noise effect that can corrupt the quality of the reconstructed images. Correlation is a well-known signal processing technique used in many applications in communications and radar systems in which the range or velocity of a target is determined by the correlation of the received scattered signal with a reference copy of the transmitted signal. In this study, we propose TR-FDTD microwave imaging combined with the cross-correlation processing to extract images from scattered signals in a noisy environment. This is entirely different than the use of cross-correlation

in typical radar signal processing where the goal there is to enable accurate measurement of range or produce range images. In our technique, cross-correlation is used to enable accurate computation of the electric and magnetic fields in very noisy environments using the TR-FDTD method. Another important contribution this paper provides is proving that processed data through correlation can still be used in the discretized Maxwell's equations to reconstruct images successfully through the FDTD method. It is also important to note that using correlated data in a noise-free environment slightly worsens the reconstructed image compared with using the original data without correlation. However, in a noisy environment the correlation / TR-FDTD method is far superior since the reconstructed images without correlation are buried in noise, as demonstrated in the results section.

Through-wall image reconstruction in the presence of added noise is used as a test case to demonstrate the efficacy and robustness of the proposed technique. However, the proposed method is also highly promising for other microwave imaging applications.

## II. ANALYSIS

### A. Time-reversed FDTD

FDTD is a numerical method for solving the differential form of Maxwell's equations to obtain the electric and magnetic fields, in both the temporal and spatial domains, by implementing the Yee algorithm [20]. The latter is based on the finite difference approximation of the time and space derivatives in Maxwell's curl equations, each of which is divided into three scalar equations in the case of three-dimensional formulation, then discretized in time and space through the use of a central difference formula in a computational domain consisting of Yee cells. The future value of both the electric and magnetic fields are updated from their previous values at each point in the grid. The propagation of the fields within the computational domain is truncated by absorbing boundaries, to mimic open space [21]. Several techniques for absorbing boundaries have been proposed, one of which is the convolutional perfectly matched layers (CPML) considered to be one of the most robust and accurate methods for truncating the computational space [22]. It is capable of absorbing evanescent and propagating waves, and can be placed close to the scattering objects resulting in a relatively compact computational space.

Time reversal algorithms have been used in other disciplines such as ultrasonic imaging applications. The same principle is applied in FDTD to reconstruct images from experimentally captured data by reversing all the FDTD update equations, so that the previous value of each field component is calculated using its future counterpart. As an example, for the time-reversed FDTD equations, the  $z$  component of the electric field  $E_z$  and

the  $y$ -component of the magnetic field  $H_y$  in the non-CPML lossy region are given in Equations (1) and (2) respectively.

$$E_z \Big|_{i,j,k+\frac{1}{2}}^n = \left( \frac{1 + \frac{\Delta t \sigma_z^e \Big|_{i,j,k+\frac{1}{2}}}{2\varepsilon_z \Big|_{i,j,k+\frac{1}{2}}}}{1 - \frac{\Delta t \sigma_z^e \Big|_{i,j,k+\frac{1}{2}}}{2\varepsilon_z \Big|_{i,j,k+\frac{1}{2}}}} \right) \times E_z \Big|_{i,j,k+\frac{1}{2}}^{n+1} - \left( \frac{\frac{\Delta t}{\varepsilon_z \Big|_{i,j,k+\frac{1}{2}}}}{1 - \frac{\Delta t \sigma_z^e \Big|_{i,j,k+\frac{1}{2}}}{2\varepsilon_z \Big|_{i,j,k+\frac{1}{2}}}} \right) \times \left[ \frac{1}{\Delta x} \left( H_y \Big|_{i+\frac{1}{2},j,k+\frac{1}{2}}^{n+\frac{1}{2}} - H_y \Big|_{i-\frac{1}{2},j,k+\frac{1}{2}}^{n+\frac{1}{2}} \right) - \frac{1}{\Delta y} \left( H_x \Big|_{i,j+\frac{1}{2},k+\frac{1}{2}}^{n+\frac{1}{2}} - H_x \Big|_{i,j-\frac{1}{2},k+\frac{1}{2}}^{n+\frac{1}{2}} \right) - J_{iz} \Big|_{i,j,k+\frac{1}{2}}^{n+\frac{1}{2}} \right] \quad (1)$$

where  $E$  is electric field intensity,  $\sigma^e$  is electric conductivity,  $\varepsilon$  is permittivity,  $J$  is electric current density,  $\Delta t$  is the time step, and  $\Delta x$ ,  $\Delta y$ , and  $\Delta z$  are the grid spacings;

$$H_y \Big|_{i+\frac{1}{2},j,k+\frac{1}{2}}^{n-\frac{1}{2}} = \left( \frac{1 + \frac{\Delta t \sigma_y^m \Big|_{i+\frac{1}{2},j,k+\frac{1}{2}}}{2\mu_y \Big|_{i+\frac{1}{2},j,k+\frac{1}{2}}}}{1 - \frac{\Delta t \sigma_y^m \Big|_{i+\frac{1}{2},j,k+\frac{1}{2}}}{2\mu_y \Big|_{i+\frac{1}{2},j,k+\frac{1}{2}}}} \right) \times H_y \Big|_{i+\frac{1}{2},j,k+\frac{1}{2}}^{n+\frac{1}{2}} - \left( \frac{\frac{\Delta t}{\mu_y \Big|_{i+\frac{1}{2},j,k+\frac{1}{2}}}}{1 - \frac{\Delta t \sigma_y^m \Big|_{i+\frac{1}{2},j,k+\frac{1}{2}}}{2\mu_y \Big|_{i+\frac{1}{2},j,k+\frac{1}{2}}}} \right) \times \left[ \frac{1}{\Delta x} \left( E_z \Big|_{i+1,j,k+\frac{1}{2}}^n - E_z \Big|_{i,j,k+\frac{1}{2}}^n \right) - \frac{1}{\Delta z} \left( E_x \Big|_{i+\frac{1}{2},j+\frac{1}{2},k+1}^n - E_x \Big|_{i+\frac{1}{2},j-\frac{1}{2},k}^n \right) - M_{iy} \Big|_{i+\frac{1}{2},j,k+\frac{1}{2}}^n \right] \quad (2)$$

where  $H$  is magnetic field intensity,  $\sigma^m$  is magnetic conductivity,  $\mu$  is permeability, and  $M$  is magnetic current density.

In the simulations, the forward FDTD equations are used to record the signals scattered by objects placed in the computational domain using a plane wave as the source signal. The recorded signals can be one or more components of the electric field at a rectangular grid corresponding to receiving antenna locations. In the image reconstruction process, the recorded signals, through simulations or measurements, are used in the TR-FDTD equations to inject the time-reversed signals back into a computational domain of only vacuum. A two-dimensional image is formed in any desired plane using the magnitude of the electric field to produce a color plot in that plane. A three-dimensional image can

be formed by concatenating 2D image slices if desired.

### B. Cross-correlation process

Cross-correlation [23] is a well-known signal processing technique used widely in communication systems as a measure of the similarity between two signals. It is mathematically represented for real signals by the following equation:

$$y(\tau) = \int_{-\infty}^{+\infty} x(t + \tau)g(t)dt, \quad (3)$$

where  $x(t)$  and  $g(t)$  are time domain signals. In radar signal processing,  $x(t)$  represents the received signal and  $g(t)$  represents a copy of the transmitted signal.

The main idea in minimizing the effect of noise on reconstructed image quality is to apply the cross-correlation process to each captured scattered signal prior to implementing the TR-FDTD method. In other words, Equation (3) is applied to all captured signals to produce cross-correlated signals, which are then used in the TR-FDTD algorithm to produce the image. Since the correlation operation quantifies the level of similarity between two signals, the hypothesis is that desired portions of the scattered signals due to the object being imaged are preserved while the noise portions of these signals are significantly diminished. The question is then: can the signals obtained after correlation still be used in the discretized TR-FDTD algorithm to improve the quality of reconstructed images? This work clearly demonstrates that the idea works very well to produce clear images using noisy signals. The substantial improvement in the image quality is due to the fact that the cross-correlation process between the captured signals and the source signal (the stored reference signal) enhances the portions of the signals that are truly scattered by the object being imaged, and at the same time, it suppresses the uncorrelated components between them (the noise). It is worth noting that in an ideal noiseless environment, the cross-correlation operation worsens the image slightly since it enhances the stronger scattering points of the image more than the weaker scattering points. In other words, it magnifies the difference between the parts of the object that are strong scatters (e.g., corners and edges) and the parts that are not as strong. This is a small price to pay in the case of a severely noisy environment since the noise renders the image totally useless without the proposed cross-correlation processing.

In our experiment, a microwave network analyzer was used to capture scattered signal in the frequency domain, and therefore, the inverse discrete Fourier Transform was applied to obtain the time domain scattered signals prior to the cross-correlation and TR-FDTD processing. In our simulations, a time domain pulse that represents a sinc-modulated sinusoid having the same bandwidth as its experimental counterpart was used for proper comparison between simulation and experimental

results.

### III. SIMULATION RESULTS

To validate the method, we simulated a model for a human body behind a drywall for a near-field microwave through-wall imaging application, as depicted in Fig. 1. The human body model was illuminated by a microwave signal and the scattered signals were recorded on a uniform rectangular grid. There are several configurations that can be used in the TR-FDTD method including monostatic, bistatic, and multistatic approaches, for both reflection and transmission systems. In this simulation example, we used a multistatic configuration in which the source was a normally incident plane wave entering the computational space from the positive  $x$  direction. The plane wave signal was a sinc-modulated sinusoidal function with a bandwidth from 8 to 12 GHz and a center frequency of 10 GHz, as shown in Fig. 2. The scattered fields, due to reflections from the wall and human body model, were recorded by capturing the  $E_z$  component at cells on a planar grid ( $yz$  plane) separated by a uniform distance equal to  $0.5\lambda$ , where  $\lambda$  is the wavelength at the highest frequency of the incident plane wave. The human body model had a height of  $8\lambda$  and a width of  $4\lambda$ , with dielectric properties of human skin ( $\epsilon_r = 36$  and  $\sigma_e = 4$ ). The body was located at a distance of  $1.2\lambda$  behind a drywall which had a thickness of  $1.2\lambda$ , a dielectric constant  $\epsilon_r = 2.19$ , and electrical conductivity  $\sigma_e = 0.0136$  S/m, similar to what is reported in the literature for this type of wall.

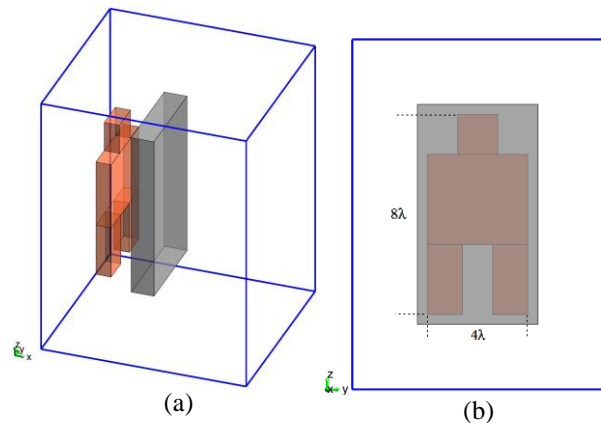


Fig. 1. (a) Perspective view and (b) front view of the original simulated object.

The reflected signals were recorded at a distance of  $5\lambda$  from the wall, a sample of the recorded signals is shown in Fig. 4 (a). All the recorded signals from the forward simulation were used in the TR-FDTD algorithm to reconstruct the image of the human body, which was done successfully as shown in Fig. 3. It is worth noting

here that the TR-FDTD computational domain was assumed to be filled with air.

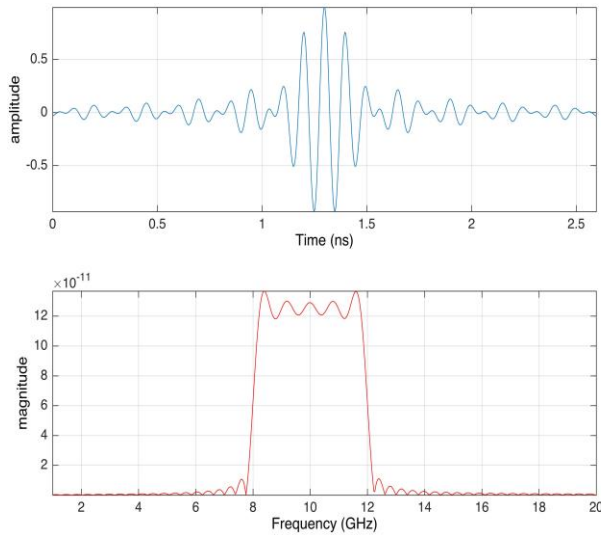


Fig. 2. Transmitted signal used in simulation and its frequency domain.

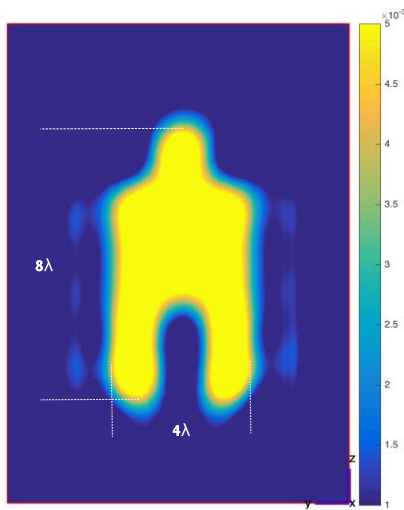


Fig. 3. Reconstructed image from the TR-FDTD algorithm.

To test the proposed technique, an interfering white Gaussian noise signal was added to the recorded signals to mimic a severe noisy environment; a sample resultant signal is shown in Fig. 4 (b). The signal-to-noise ratio (SNR), in this case, varied from  $-1.6$  dB to  $-28.9$  dB, due to the fact that the collected signals on the planar grid have varying strengths depending on their location with respect to the scattering object. For example, signals near the center of the planar grid have higher average signal power than those near the corners of the grid. Consequently, SNR varies since the numerically added

noise power is constant regardless of the signal's location on the grid. Plugging these corrupted signals into the TR-FDTD algorithm resulted in a severely distorted image, as shown in Fig. 5 (a). To minimize the noise from the recorded signal, cross-correlation processing was applied between all the recorded signals and a copy of the transmitted signal; a sample signal after cross-correlation is shown in Fig. 4 (c). Using the cross-correlated signals as inputs to the TR-FDTD algorithm led to the successful reconstruction of the original image. Figure 5 (b) shows the reconstructed image using the cross-correlated signals. As clear from the figure, the improvement in image quality using the proposed method is remarkable.

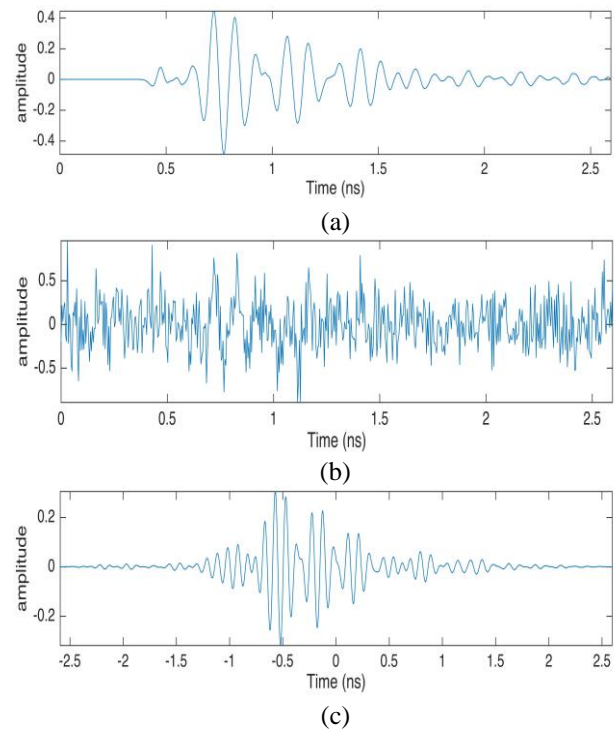


Fig. 4. Sample captured signal from the simulation: (a) in the absence of interfering noise, (b) with added noise, and (c) after cross-correlation of the corrupted signal.

#### IV. EXPERIMENTAL RESULTS

The proposed technique was tested experimentally using a monostatic configuration for a near-field reflection system. A single small horn antenna (aperture dimensions  $4.5 \times 3.0$  cm) was simultaneously used as a transmitter and receiver. The antenna was moved on a uniform planar grid ( $20 \times 30$  cm) with grid spacing of 1.25 cm which corresponds to half wavelength at the highest frequency used in the measurement (12 GHz). This grid spacing resulted in  $16 \times 24$  antenna locations for a total of 384 captured signals. A network analyzer was used as the transmitter source and receiver. The frequency domain scattering parameter  $S_{11}$  was recorded at each

antenna location using the frequency range 8-12 GHz (identical to the frequency range used in the simulations). The inverse discrete Fourier transform was then used to convert all the captured  $S_{11}$  signals to the time domain.

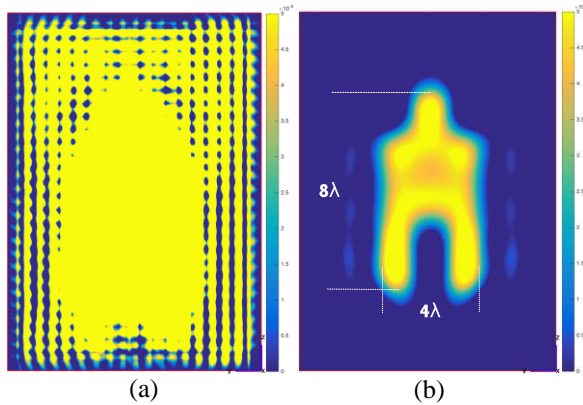


Fig. 5. Reconstructed image using: (a) the corrupted signal and (b) the cross-correlated data.

A human body model, made of conducting material with exactly the same dimensions as in the simulation case, was placed behind a wall for the measurement. The wall used was made with drywall, 2 × 4 wood studs, and OSB board for a total thickness of 11 cm; it was located 5 cm away from the planar grid, as shown in Fig. 6.

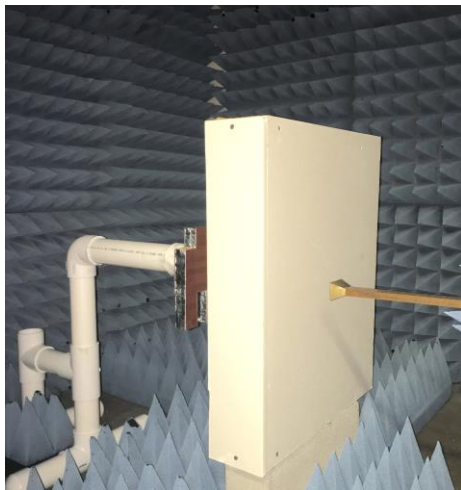


Fig. 6. Experimental setup for near-field through-wall microwave imaging of a human body model.

The time-domain transmitted (source) signal, after conversion to the time domain, is shown in Fig. 7. One sample of the scattered signals captured by the antenna is shown in Fig. 9 (a). All the signals captured by the antenna at the 384 grid locations were used in the TR-FDTD algorithm to reconstruct the image of the human body model. The image obtained resembles the original

object very closely, as shown in Fig. 8.

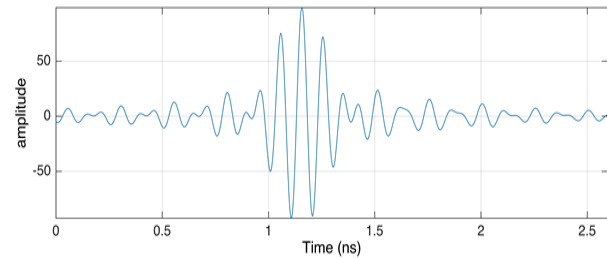


Fig. 7. Experimental transmitted signal in the time domain.

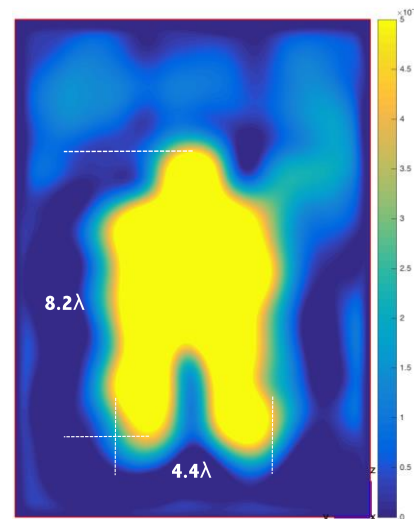


Fig. 8. Reconstructed image using experimental data.

We repeated the same scenario as in the simulation case of strong noise interference by adding an interfering noise signal to the measurements. The SNR was between -0.014dB and -6.28dB; a sample noisy signal is shown in Fig. 9 (b). It is worth noting that the noise signal used here is an experimental noise with a bandwidth limited to the bandwidth of the horn antenna, which was in the range of 8-12 GHz. The signals corrupted with noise were used in the TR-FDTD algorithm to reconstruct the image; the image obtained was unrecognizable, as shown in Fig. 10 (a).

We then applied the cross-correlation process prior to the TR-FDTD image reconstruction process. A sample signal after the cross-correlation process is shown in Fig. 9 (c). All the cross-correlated signals were then used in the TR-FDTD algorithm for image reconstruction. As shown in Fig. 10 (b), the noise was substantially minimized and the image obtained closely resembles the original object. The images shown in the figure clearly demonstrate the remarkable capability of the proposed method in minimizing the effect of noise in image reconstruction. It is worth noting that all the images are

raw images reconstructed using the proposed technique without any post-processing enhancement.

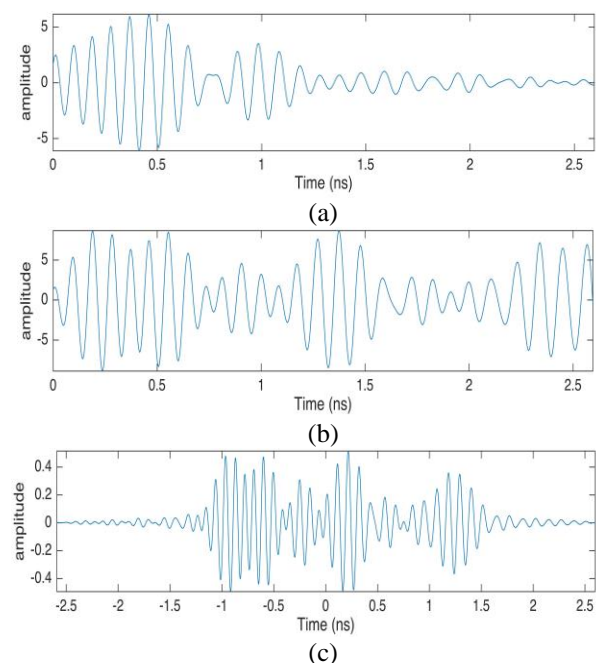


Fig. 9. Sample captured signal from the experiment: (a) in the absence of interfering noise, (b) with added noise, and (c) after cross-correlation of the corrupted signal.

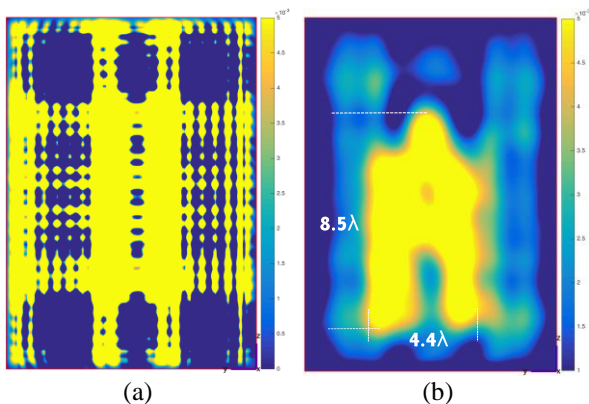


Fig. 10. Image reconstructed from: (a) the corrupted signal and (b) the cross-correlated data.

## V. CONCLUSION

A new microwave imaging method combining the time-reversed finite-difference time-domain method (TR-FDTD) with cross correlation processing to minimize the effect of noise was presented. An x-band (8–12 GHz) reflection setup was used to reconstruct images using data corrupted with large amount of noise. Captured signals scattered by the object were cross-correlated with a copy of the transmitted signal prior to processing using the TR-FDTD method. Our behind the wall imaging

simulations as well as experiments demonstrated the power of the proposed method. The combined TR-FDTD and cross-correlation technique successfully produced clear images, while the standard TR-FDTD method produced severely distorted images that bear no resemblance to the actual object.

## REFERENCES

- [1] L. Giubbolini, "A microwave imaging radar in the near field for anti-collision (MIRANDA)," *IEEE Transactions on Microwave Theory and Techniques*, vol. 47, no. 9, pp. 1891-1900, Sep. 1999.
- [2] Y. Wang, A. M. Abbosh, B. Henin, and P. T. Nguyen, "Synthetic bandwidth radar for ultra-wideband microwave imaging systems," *IEEE Transactions on Antennas and Propagation*, vol. 62, no. 2, pp. 698-705, Feb. 2014.
- [3] M. Peichl, S. Dill, M. Jirousek, and H. Suess, "Near-field microwave imaging radiometers for security applications," *7th European Conference on Synthetic Aperture Radar (EUSAR)*, Friedrichshafen, Germany, 2008.
- [4] M. Klemm, J. A. Leendertz, D. Gibbins, I. J. Craddock, A. Preece, and R. Benjamin, "Microwave radar-based breast cancer detection: Imaging in inhomogeneous breast phantoms," *IEEE Antennas and Wireless Propagation Letters*, vol. 8, pp. 1349-1352, 2009.
- [5] E. C. Fear, J. Bourqui, C. Curtis, D. Mew, B. Docktor, and C. Romano, "Microwave breast imaging with a monostatic radar-based system: A study of application to patients," *IEEE Transactions on Microwave Theory and Techniques*, vol. 61, no. 5, pp. 2119-2128, May 2013.
- [6] M. Klemm, J. A. Leendertz, D. Gibbins, I. J. Craddock, A. Preece, and R. Benjamin, "Microwave radar-based differential breast cancer imaging: Imaging in homogeneous breast phantoms and low contrast scenarios," *IEEE Transactions on Antennas and Propagation*, vol. 58, no. 7, pp. 2337-2344, July 2010.
- [7] K. M. Yemelyanov, N. Engheta, A. Hoorfar, and J. A. McVay, "Adaptive polarization contrast techniques for through-wall microwave imaging applications," *IEEE Transactions on Geoscience and Remote Sensing*, vol. 47, no. 5, pp. 1362-1374, May 2009.
- [8] F. Ahmad, M. G. Amin, and S. A. Kassam, "Synthetic aperture beamformer for imaging through a dielectric wall," *IEEE Transactions on Aerospace and Electronic Systems*, vol. 41, no. 1, pp. 271-283, Jan. 2005.
- [9] E. C. Fear, X. Li, S. C. Hagness, and M. A. Stuchly, "Confocal microwave imaging for breast cancer detection: Localization of tumors in three dimensions," *IEEE Transactions on Biomedical*

- Engineering*, vol. 49, no. 8, pp. 812-822, Aug. 2002.
- [10] M. Elsdon, M. Leach, S. Skobelev, and D. Smith, "Microwave holographic imaging of breast cancer," *International Symposium on Microwave, Antenna, Propagation and EMC Technologies for Wireless Communications*, Hangzhou, 2007.
- [11] G. Lerosey, J. de Rosny, A. Tourin, A. Derode, G. Montaldo, and M. Fink "Time reversal of electromagnetic waves," *Physical Review Letters*, vol. 92, 193904, May 2004.
- [12] M. Fink, D. Cassereau, A. Derode, C. Prada, P. Roux, M. Tanter, J. L. Thomas, and F. Wu, "Time-reversed acoustics," *Reports on Progress in Physics*, vol. 63, pp. 1933-1995, 2000.
- [13] M. E. Yavuz and F. L. Teixeira, "A numerical study of time-reversed UWB electromagnetic waves in continuous random media," *IEEE Antennas and Wireless Propagation Letters*, vol. 4, pp. 43-46, 2005.
- [14] A. E. Fouda, F. L. Teixeira, and M. E. Yavuz, "Imaging and tracking of targets in clutter using differential time-reversal," *Proceedings of the 5th European Conference on Antennas and Propagation (EUCAP)*, Rome, pp. 569-573, 2011.
- [15] P. Kosmas and C. M. Rappaport, "Time reversal with the FDTD method for microwave breast cancer detection," *IEEE Transactions on Microwave Theory and Techniques*, vol. 53, no. 7, pp. 2317-2323, July 2005.
- [16] C. Bardak and M. Saed, "Microwave imaging with a time-reversed finite-difference time-domain technique," *Journal of Electromagnetic Waves and Applications*, vol. 28, no. 12, 2014.
- [17] W. Zheng, Z. Zhao, and Z. Nie, "Application of TRM in the UWB through wall radar," *PIER*, vol. 87, pp. 279-296, 2008.
- [18] L. Li, W. Zhang, and F. Li, "A novel autofocusing approach for real-time through-wall imaging under unknown wall characteristics," *IEEE Transactions on Geoscience and Remote Sensing*, vol. 48, no. 1, pp. 423-431, Jan. 2010.
- [19] A. B. Gorji and B. Zakeri, "Time-reversal through-wall microwave imaging in rich scattering environment based on target initial reflection method," *ACES Journal*, vol. 30, no. 6, June 2015.
- [20] K. S. Yee, "Numerical solution of initial boundary value problems involving Maxwell's equations in isotropic media," *IEEE Transaction on Antennas and Propagation*, vol. 14, pp. 302-307, 1966.
- [21] A. Z. Elsherbeni and V. Demir, *The Finite-Difference Time-domain Method for Electromagnetics with Matlab Simulations*. SciTech Publishing, 2009.
- [22] J. A. Roden and S. D. Gedney, "Convolution PML (CPML): An efficient FDTD implementation of

the CFS-PML for arbitrary media," *Microwave and Optical Technology Letters*, vol. 27, pp. 334-339, 2000.

- [23] J. G. Proakis and D. K. Manolakis, *Digital Signal Processing*. 4th Edition, Pearson, 2007.



**Ayed R. Alajmi** received the B.S. and M.S. degrees from Kuwait University, Kuwait, in 2003 and 2008, respectively, and the Ph.D. degree in Electrical Engineering from Texas Tech University, Lubbock, Texas in 2017. From 2007 to 2010, he was a Teacher at The Higher Institute of Telecommunications and Navigation, Kuwait. Since February 2010, he has been a Faculty Member in the Department of Electronics Engineering, College of Technological Studies, Public Authority for Applied Education and Training in Kuwait. His research interests include electromagnetic waves propagation, computational electromagnetics, microwave imaging and nanotechnology in electronic and communication systems.



**Mohammad A. Saed** received the B.S. degree in Electrical Engineering from Middle East Technical University, Ankara, Turkey in 1983, and the M.S. and Ph.D. degrees in Electrical Engineering from Virginia Tech, Blacksburg, in 1984 and 1987, respectively. From 1989 to 1990, he was a Research Associate at Virginia Tech. In 1990, he joined the faculty of the Electrical Engineering Department of State University of New York, New Paltz. In 2001, he joined the Electrical and Computer Engineering Department of Texas Tech University, Lubbock, where he is currently an Associate Professor. His research interests include applied electromagnetics with emphasis on microwave imaging and sensing, computational electromagnetics, antennas, and microwave and terahertz components and applications.